

Fast Defect Detection for Various Types of Surfaces using Random Forest with VOV Features

Bae-Keun Kwon¹, Jong-Seob Won², and Dong-Joong Kang^{1#}

¹ School of Mechanical Engineering, Pusan National University, 2, Busandaehak-ro 63beon-gil, Geumjeong-gu, Busan, 609-735, South Korea

² Department of Mechanical & Automotive Engineering, Jeonju University, 303, Cheonjam-ro, Wansan-gu, Jeonju-si, Jeollabuk-do, 560-759, South Korea

Corresponding Author / E-mail: djkgang@pusan.ac.kr, TEL: +82-51-510-2356, FAX: +82-51-514-1118

KEYWORDS: Defect detection, Surface inspection, Random forest, Machine learning

Defect detection on an object surface is one of the most important tasks of an automated visual inspection system. The most modern defect detection systems are required to operate in real-time and handle high-resolution images. One of main difficulties in system applications is that it cannot be used for general inspection of various types of surface without tuning the internal parameters. In this paper, we demonstrate how to solve the problem mentioned above by using simple variance profile values of pixel intensities and applying it to the random-forest-based machine learning algorithm. Variance of Variance (VOV) profiles are used to describe the texture of an object surface and to amplify the irregularity of intensity variations. The feature amplification property of the VOV method can be applied generally to various types of surface and defect. For effective learning and reduction of false detection, a defect-size insensitive approach and a hard sample retraining process are introduced. The experimental results demonstrate reliable defect detection for various surface types without changing parameters.

Manuscript received: November 12, 2014 / Revised: February 17, 2015 / Accepted: February 26, 2015

1. Introduction

Automated defect detection using a vision system is one of core technologies for improvement in the productivity and maintenance of high product quality in a factory. Methods of detecting defects on surfaces in diverse conditions have been developed through many studies in the last decade, and the result of the related studies has been used as one of inspection tools being applied to actual systems. One of the representative methods related to defect detection is to detect defects using Independent Component Analysis (ICA), which analyzes main components of the pixel's intensity (i.e., brightness) variations of a surface. The method using ICA is the most common for weak defects such as a wafer with low contrast¹⁻³ and the studies on detection of defects on planes with more diverse textures⁴ have been reported as the main result. Also, a method of finding defects by analyzing the texture or frequency of a defect has been studied,⁵ and studies on detection of defects on different backgrounds such as wood,⁶ fabric,⁷⁻⁹ and metal¹⁰ have been in progress. As defect images are taken with the various features of the background on them, the types of defect may be diversely expressed with a wide spectrum in size from small defects such as dust and ink-drop to big ones such as scratches, pin-holes, and oil-pollution. The works presented by many researchers show that high detection

performance was made when a specific method was applied to each of different surface types. However, different methods should be selected whenever the type of background changes due to different features appearing on diverse surfaces. Furthermore, depending on the change in the defect size, the inspection performance has been found to be deteriorated in many cases. Accordingly, the demand for a general detection method that can be used on diverse types of background containing diverse defects is increasing.

The main contribution of the paper is to propose a simple but unique defect detection method that can be applied to inspect diverse types of defect on diverse surfaces. The method proposed utilizes features of the defect and background in terms of Variance of Variance (VOV) where simple information about variance of pixel intensities is used, and with which it is intended to differentiate defects from the background through a random forest¹¹ based classifier. Also, a retraining process for false classifications is applied to enhance the training performance.¹²

2. VOV Features

2.1 Modeling VOV features

A good feature in defect detection is thought to be the one that

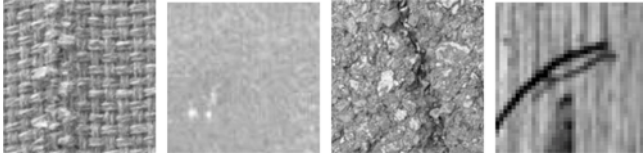


Fig. 1 Various Types of Surfaces and Defects

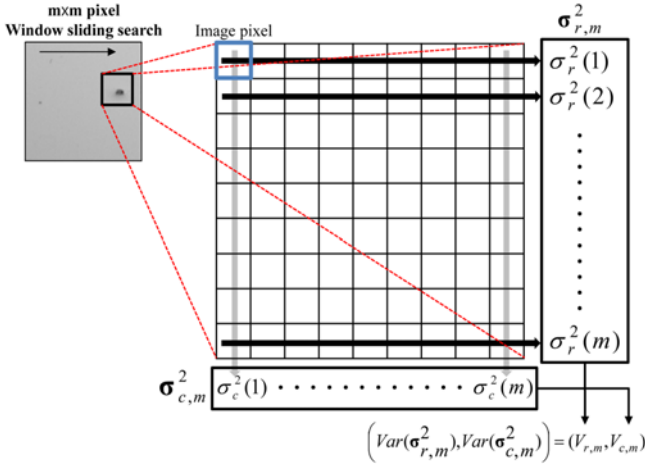


Fig. 2 Definition of VOV

clearly differentiates a defect from the background. The feature most widely used in a defect inspection process in the past was a frequency of intensity, which is used as a representative value indicating the changing rate in pixel intensity and differentiating the defect from the background. Also, the frequency feature was used for defect detection through versatile applications such as ICA and wavelet filters. However, the main disadvantage of frequency feature is that, the more the surfaces and objects are diversified, the more difficult it becomes to use it as a feature because the frequency boundary becomes imprecise.

The Haar-like feature is one of the most famous features. Also, many researchers have used it for object detection with the adaptive-boosting algorithm.¹³ However, it needs additional processing like local intensity normalization on a non-uniform background, and it is not easy to use it on surfaces with texture and/or gradation. In light of these, in this paper, VOV is employed as the representative feature that expresses the change in background textures.

Though simple, VOV takes the role of amplifying variation of intensity. With VOV, it is possible to find defects through irregular changes different from the background. Accordingly, it enables discrimination of defects by amplifying a small difference in the change in intensity between the background and the defect into a large difference in VOV value.

The definition of VOV and its calculation process are given in Fig. 2. Let $x(i, j)$ be the intensity value of a pixel located in the i^{th} row and the j^{th} column in a partial image (sampled and taken from an entire image) of size $m \times m$. To proceed, let us begin with the pixels placed in a row on the image. For the intensity value of each pixel in the i^{th} row, its variance can be calculated as shown in Eq. (1). The subscript r (c , shown in later) denotes the row (column) in the image at hand.

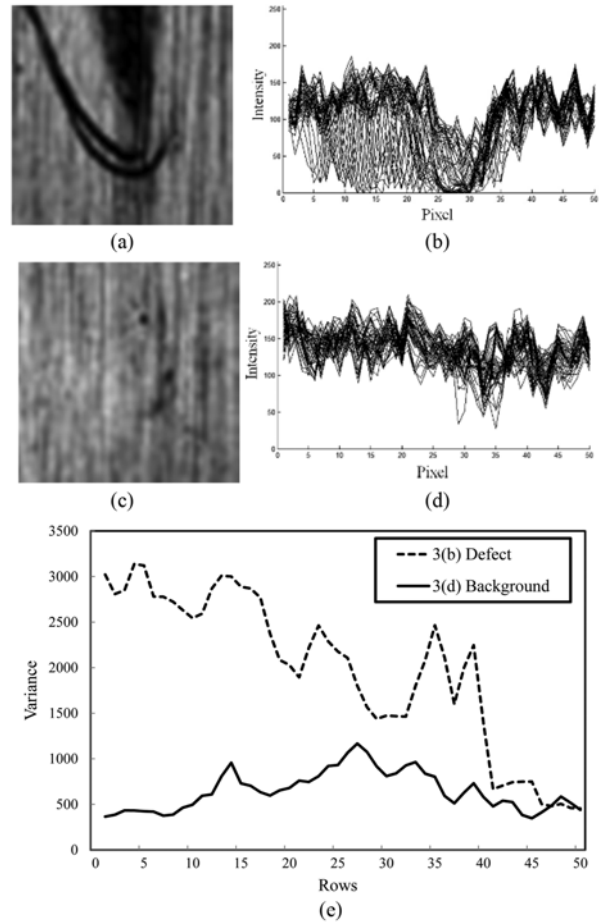


Fig. 3 Variance profiles of intensity values obtained from the horizontal direction calculation for two sample images: (a) Image containing defects, (b) Intensity profiles for the image in (a), (c) Image without defects, (d) Intensity profiles for the image in (c), and (e) Profiles of VOVs from (b) and (d)

$$\sigma_r^2(i) = Var(\mathbf{x}_r(i)) = \frac{1}{m} \sum_{j=1}^m x(i, j)^2 - \bar{x}_r(i)^2 \quad (1)$$

where $\mathbf{x}_r(i) = \{x(i, j) | \forall j\}$ is a set of the intensity values of the pixels in the i^{th} row, and $\bar{x}_r(i)$ represents the mean value of $\mathbf{x}_r(i)$. A set having variance values for each row as its element is defined in Eq. (2).

$$\sigma_{r,m}^2 = \{\sigma_r^2(1), \dots, \sigma_r^2(m)\} \quad (2)$$

Using the elements of the variance set defined above, a new variance value can be calculated and is called the VOV in the row direction (row-VOV, briefly and denoted by $V_{r,m}$). With the similar manner, the VOV in the column direction (column-VOV, briefly and denoted by $V_{c,m}$) can be obtained.

$$[Var(\sigma_{r,m}^2), Var(\sigma_{c,m}^2)] = [V_{r,m}, V_{c,m}] \quad (3)$$

In the following, an illustrative example for finding VOV is given. Figs. 3(a) and (c) present two sample images with the size of 50 by 50 pixels, respectively. The first image is taken from a region containing defects on a wooden surface, and the second from the surrounding region having minor defects. This first (second) image is referred to as

defect (background) for brevity, hereafter.

From the first image, the intensity of respective pixel arrayed at each row was extracted and its intensity profile for each row is given in Fig. 3(b). With the same manner, the intensity profile for the second image is given in Fig. 3(d). It is observed from the Figs. 3(b) and (d) that the intensity distribution of the defect is more scattered than that of the background, since the dark color features in the defects.

Variance of intensity values (of pixels) per each row in the sample image was calculated via Eq. (1) for each data set expressed in Figs. 3(b) and (d). Their profiles are given in Fig. 3(e), where the dotted line denotes the variance set for the defect image and the solid line for the background image.

As shown in the plot, the magnitude of variance in the image of Fig. 3(a) is bigger than that of Fig. 3(c) for the majority of the section except for a few rows due to the difference in the intensity between the background and the defect. For calculation of mean and variance, the integral image method is known to be very fast solution.¹⁴

Variance denotes the degree of scatteredness of sampling data. Likewise, variance of variance measures how far a set of data having values of variance is spread out. As shown above, the defect has higher VOV than the background, as the spread of variance in the defect is bigger than that in the background. The main character of VOV is to summarize the distribution values of intensity into a single value.

The condition to be good feature in general detection methods is in versatile expressions and simple calculation. Structural information on a defect can be a good feature for a similarly shaped defect; however, it needs too much information in proportion to the number of defect types. The method employing VOV, which is proposed in this work, provides a significant difference from the existing detection methods in the point that in spite of its simplicity, it can express defects, irrespective of the background type. Additionally, it can skip the local intensity normalization, and is strong for illumination changes, because variance can be expressed from the average of intensity on a local window. Also, a defect-size insensitive approach is incorporated to handle the changeable types of defect for different sizes and textures. Consequently, high performance on defect detection can be achieved by using a learning algorithm based on VOV properties.

2.2 Defect direction and window size

The employment of VOV, as a whole, shows high classification performance without depending on the types of background. But, performance deterioration can also be occurred depending on the defect size and the direction of the background texture. Accordingly, the inspection error can be reduced by employing features with different window sizes and directions.

In Fig. 4, the VOV values for the same image are expressed using two different window sizes. The employment of a small window size can be feasible to extract small size defects; however, for the background with big texture like wood, it is not easy to be used since the background can be recognized as defects. Although, on the other hand, the use of a big window size makes it possible to extract best a defect with big texture, it is not a trivial task to extract small defect with small texture. Thus, it can be seen that defects can be expressed only when the window size is changed in proportion to the texture size of the background.

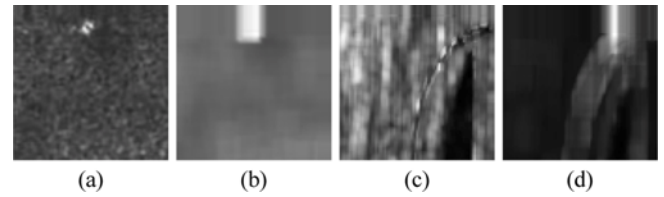


Fig. 4 Images of VOV values for two different window sizes: (a) Car surface with $w=5$, (b) Car surface with $w=15$, (c) Wood surface with $w=5$, and (d) Wood surface with $w=15$. Note: w is the window size

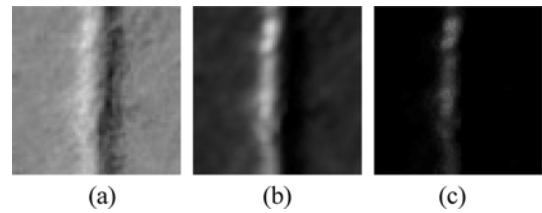


Fig. 5 Example images showing the directional characteristic of VOV: (a) Original Image, and images from the application of (b) Row-VOV and (c) Column-VOV, respectively. Note: The window size is set to 5

The VOV value has directionality. This characteristic can be explained in Fig. 5. Fig. 5(a) is an original image that shows the defect placed lengthwise. The VOV value obtained through the variance values in the horizontal direction is given in Fig. 5(b). With the same manner, the VOV value through the variance values in the vertical direction is given in Fig. 5(c). It is observed from the figures that the row-VOV gives more apparent results than the column-VOV. The directionality of a defect can also be considered by using the row-VOV and column-VOV values together. In this paper, a parameter describing the size of defect is defined as the product of the row- and column-VOVs as shown in Eq. (4), and is called the VOV parameter:

$$\omega(w) = V_{r,w} \times V_{c,w} \quad (4)$$

where $\omega(w)$ is the VOV parameter, and w is the window size. As already mentioned before, $V_{r,w}$ and $V_{c,w}$ denote the row- and column-VOVs, respectively. Note that the VOV parameter is the function of the window size w . In Eq. (5), the optimum window size is represented as one where the VOV difference between the defect image and the background image is maximized.

$$w_r = \operatorname{argmax}_w |\omega_{defect}(w) - \omega_{back}(w)| \quad (5)$$

where $\omega_{defect}(w)$ and $\omega_{back}(w)$ are the VOV parameter of the defect image and the background image, respectively.

3. Random Forests

Several features can be created from VOV values using different window sizes and directions. Using a feature vector \mathbf{f} created in this way, classifiers in a classification method can be trained to recognize defects. Adaptive-boosting and random ferns¹⁵ are one of the most commonly used classification methods. Also, random forests are one

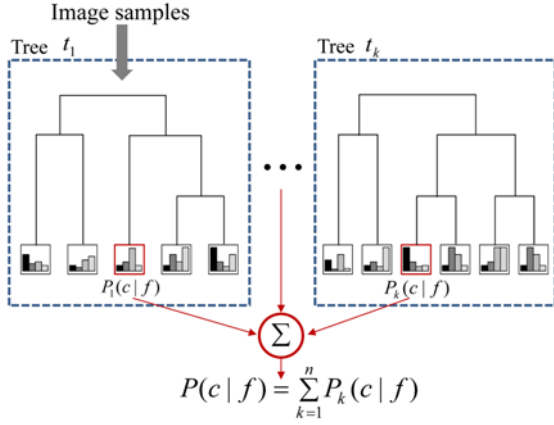


Fig. 6 Random forest process

kind of supervised learning algorithms, and can carry out fast classification using diverse features. Although adaptive-boosting and random ferns show good classification performance,¹⁶⁻¹⁸ random forests are chosen to be utilized in the work with the following reasons. First, in terms of size in feature vectors, random forests can show outstanding performance even for feature vectors with small dimensions. In this work, for instance, we defined only 24 dimensional feature vectors (i.e., $\mathbf{f} \in \mathbb{R}^{24}$). It may not be enough in size for adaptive-boosting and random ferns. Second, as already known, adaptive boosting is one of binary classifiers and many classes in feature space can decrease classification reliability. Also, binary features generated by random ferns cannot work clearly on various surfaces, since intensity comparisons of binary features can increase confusedness between surface patterns and defects. However, random forests are able to solve this problem by classifying features into classes based on types of surface. In this work, various types of surface and defect are considered, and training data sets, whose elements are not distributed continuously, are used. In light of these, random forests are adopted in this work.

Fig. 6 describes the training process of random forests, which shows the branches that appropriately classify the input feature at each node of the t^{th} binary tree. A threshold value at each node that is compared with a feature value is also given to separate effectively the defect and background training samples. The threshold is usually selected to minimize the entropy of the feature vector of each side samples after division of training samples into two sides.¹⁹⁻²¹

The bottommost node classified is called the leaf node. During training, the class probability of a leaf node is built by the bin counter increase for labeled samples which reach to this node. The number of bins in the leaf node equals to the number of classes. After training, each leaf node has the class probability by normalizing the bin count values. During test, an input sample reaches a leaf node in each tree and the leaf node suggests probability of each class. If we sum up the class probability $P_k(c|f)$ for all trees, then the class with maximum probability $P(c|f)$ is selected. For defect detection, two classes of defect and background are allowed. (See Eq. (7).)

$$P(c|f) = \sum_{k=1}^n P_k(c|f), \quad n = \# \text{ of trees} \quad (6)$$

$$\text{if } P(c_{\text{defect}}|f) > P(c_{\text{background}}|f) \text{ then defect else background} \quad (7)$$

One of the most important task in defect detection is to define a feature vector whose elements can be used to differentiate (and/or extract) common characteristics from training samples. The training samples consist of the defect and background data taken from different surfaces of diverse objects. In this work, we define and propose a 24 dimensional feature vector $\mathbf{f} = [f_1, \dots, f_{24}]$. The feature vector consists of two basic feature groups such as 16 original VOV features according to size and direction of defect and 6 application features of VOV. If we use more features, the performance of detection may increase, but it need more execution time. For tradeoff of performance and speed, features are limited to 24 types. The elements of the proposed vector are explained in the following. f_1 and f_2 represent the values of pixel intensity and strength of Canny edge²² at the center of a sliding window, respectively. $f_{3, \dots, 6}$ has the average responses of VOV values obtained when the two window patches having a large difference in size each other are applied (See Eq. (8)).

$$f_{[3, \dots, 6]} = \{\bar{V}_{r,w}, \bar{V}_{c,w}, \bar{V}_{r-\text{sol}}, \bar{V}_{c,w_{r-\text{sol}}}, \bar{V}_{r-\text{tex}}, \bar{V}_{c,w_{r-\text{tex}}}\} \quad (8)$$

where $\bar{V}_{r,w} = 1/N \sum V_{r,w}$. In this work, surfaces under consideration is divided into two groups - the solid and texture surfaces. In order to take the characteristics of surfaces into consideration, the VOV parameter of each surface is incorporated, respectively.

$$f_{[7,8]} = \{\omega(w_{r-\text{sol}}), \omega(w_{r-\text{tex}})\} \quad (9)$$

where $\omega(\bullet)$ is the VOV parameter introduced in Eq. (4). $w_{r-\text{sol}}$ ($w_{r-\text{tex}}$) denotes the optimal window size on a solid background with weak texture (on a surface with strong texture). In the work, $w_{r-\text{sol}}=5$ and $w_{r-\text{tex}}=13$, which are obtained from experiments and calculated via Eq. (5). The remainder is as follows:

$$f_{[9, \dots, 16]} = \{V_{r,w}, w=3, 5, 7, 11, 13, 15, 19, 21\} \quad (10)$$

$$f_{[17, \dots, 24]} = \{V_{c,w}, w=3, 5, 7, 11, 13, 15, 19, 21\} \quad (11)$$

Note that $f_{[9, \dots, 24]}$ includes VOV features, where the different window sizes (such as small, medium, and large) are applied depending on the background texture.

4. Experimental Results

In this paper, the experiments were carried out using 7 representative surfaces, such as wafer, solid car surface, pear color car surface, paper, fabric, stone and striped-metal, for inspection of diverse surfaces. The proposed method was implemented using C++ language on an Intel® i5 desktop.

In order to perform training process, total of 2,100 images - 300 images (200 defect images and 100 background images) per each surface, were prepared. Training has been conducted through total of 28,000 samples. Sample data consist of the positive and negative patches (each of which is a small part image and characterized as one whether having defects or not.) at the same rate. For each surface, total of 4,000 patches are considered. Among them, 2,000 positive patches are picked out from the defect images (10/image * 200 images). Similarly, 2,000 negative patches are chosen from the defect images (5/image * 200

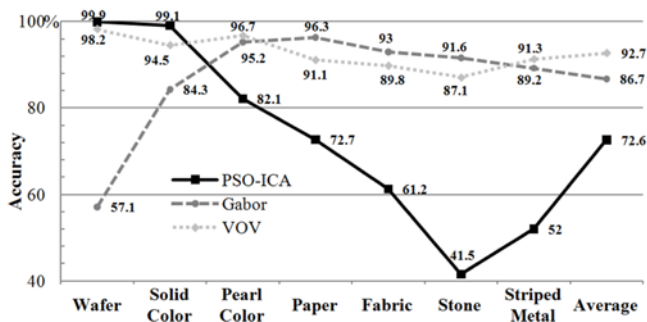


Fig. 7 Defect detection rates for various types of background

images) and the background images (10/image * 100 images).

For improvement on training performance, it is required to apply the same training sample ratio to a learning process for inspection of defects and backgrounds. Note that it took about 13 minutes for calculation in the initial training. For a verification process, another 1,000 images of 640×480 pixels, which were not participated in training, were used.

Though random forests can classify many samples in fast computation and guarantee high reliability, many errors may occur. Also, as 24-dimensional features are used for inspection of diverse surfaces and it has a defect range of diverse categories, the classification error is relatively high. Accordingly, in this paper, the classification performance was enhanced through the retraining process.^{12,13} The retraining process is a method of enhancing the classification performance by repeating re-training after analyzing the result of the initial training, and by adding false alarms and missed defects, and thus it can enhance defect detection performance.

In order to compare detection reliability, experiments have been conducted using PSO-ICA² that is well known for wafer inspections,²³ and Gabor filter¹⁰ which has high reliability for inspection of backgrounds with much texture. The results have also been compared. Figs. 7 and 8 show the results from the comparative experiments. While ICA shows very high performance for a wafer of low-contrast, the performance is shown to be deteriorated due to irregularity of the background intensity as the texture becomes complicated. Though Gabor filter has excellent performance as a whole, it lacks classification performance on a wafer where the difference in contrast between the background and the defect is very small. The proposed VOV method shows high performance in average on diverse surfaces, and it can detect all most of defects. VOV provides a consistent framework that can be used without parameters tuning for defect images with different backgrounds. Fig. 9 shows the result using VOV, which indicates the applicability of VOV to defect detection.

5. Conclusions

This paper proposes a general defect detection method which can be used on different textures of diverse backgrounds without changing the internal parameters. The employment of VOV, which is effective to differentiate defects from the background irrespective of the background type, was presented. For defects of even various sizes on diverse background textures, the VOV method is capable of detecting them in

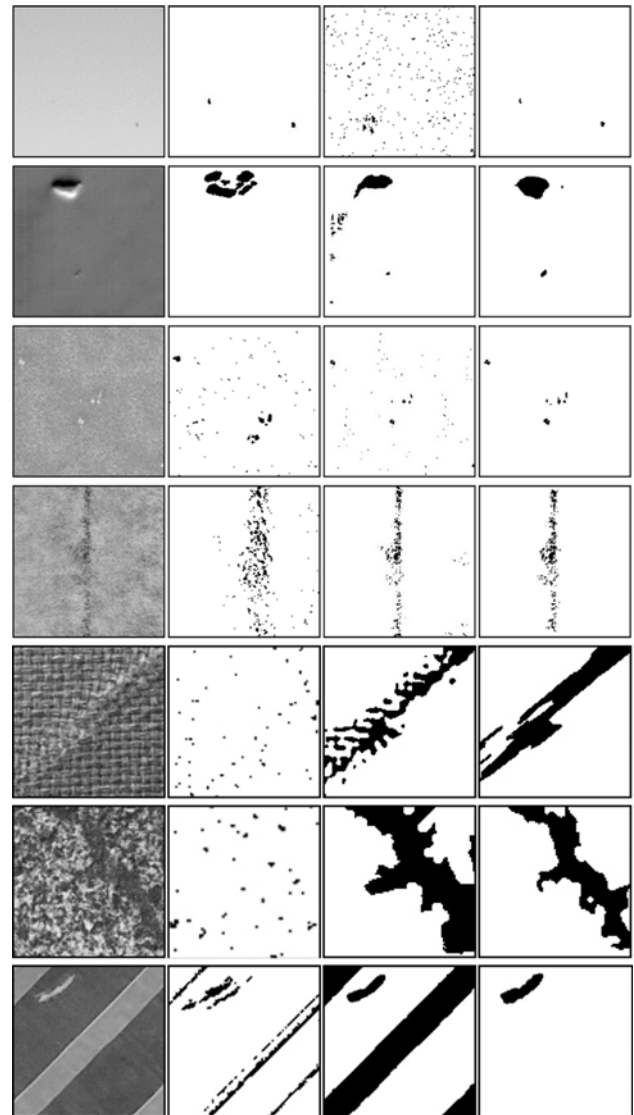


Fig. 8 Experimental results for various surfaces from different methods: (a) Original image (1st column), (b) PSO-ICA (2nd column), (c) Gabor Filter (3rd column), and (d) VOV (4th column). Note: Original images used in the experiment are taken from a surface of wafer, solid color, pearl color, fabric, stone, and striped-metal in the order shown

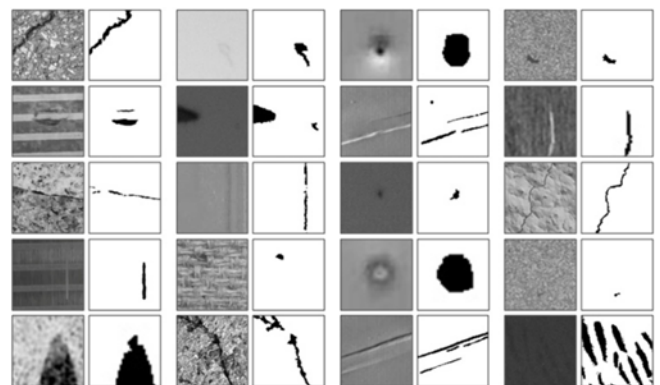


Fig. 9 Examples of defect detection for various types of background and defect

a single framework. Training was carried out using random forests that enable defect inspections to be conducted at a high speed. It is found from experiments that learning error has been reduced during the training and high performance has been realized through retraining processes. Furthermore, it is observed that low level image features are calculated with the integral image method to satisfy the real-time requirement.

ACKNOWLEDGEMENT

We would like to acknowledge the financial support from the Basic Science Research Program through NRF funded by the Ministry of Education, Science and Technology (No. 2013R1A1A2060427, No. 2011-0017228).

REFERENCES

1. Tsai, D. M., Lin, P. C., and Lu, C. J., "An Independent Component Analysis-based Filter Design for Defect Detection in Low-Contrast Surface Images," *Pattern Recognition*, Vol. 39, No. 9, pp. 1679-1694, 2006.
2. Tsai, D. M., Tseng, Y. H., Chao, S. M., and Yen, C. H., "Independent Component Analysis based Filter Design for Defect Detection in Low-Contrast Textured Images," *Proc. of International Conference on Pattern Recognition*, Vol. 2, pp. 231-234, 2006.
3. Tsai, D. M. and Lai, S. C., "Defect Detection in Periodically Patterned Surfaces Using Independent Component Analysis," *Pattern Recognition*, Vol. 41, No. 9, pp. 2812-2832, 2008.
4. Sezer, O. G., Ertizun, A., and Erçil, A., "Independent Component Analysis for Texture Defect Detection," *Pattern Recognition and Image Analysis*, Vol. 14, No. 2, pp. 303-307, 2004.
5. Jasper, W. J., Garnier, S. J., and Potlapalli, H., "Texture Characterization and Defect Detection using Adaptive Wavelets," *Optical Engineering*, Vol. 35, No. 11, pp. 3140-3149, 1996.
6. Funck, J. W., Zhong, Y., Butler, D. A., Brunner, C. C., and Forrer, J. B., "Image Segmentation Algorithms Applied to Wood Defect Detection," *Computers and Electronics in Agriculture*, Vol. 41, No. 1, pp. 157-179, 2003.
7. Serdaroglu, A., Ertuzun, A., and Erçil, A., "Defect Detection in Textile Fabric Images using Wavelet Transforms and Independent Component Analysis," *Pattern Recognition and Image Analysis*, Vol. 16, No. 1, pp. 61-64, 2006.
8. Yang, W., Li, D., Zhu, L., Kang, Y., and Li, F., "A New Approach for Image Processing in Foreign Fiber Detection," *Computers and Electronics in Agriculture*, Vol. 68, No. 1, pp. 68-77, 2009.
9. Chan, C. H. and Pang, G. K., "Fabric Defect Detection by Fourier Analysis," *IEEE Transactions on Industry Applications*, Vol. 36, No. 5, pp. 1267-1276, 2000.
10. Kumar, A. and Pang, G. K., "Defect Detection in Textured Materials using Gabor Filters," *IEEE Transactions on Industry Applications*, Vol. 38, No. 2, pp. 425-440, 2002.
11. Briman, L., "Random Forests," *Machine Learning*, Vol. 45, No. 1, pp. 5-23, 2001.
12. Caruana, R., Karampatziakis, N., and Yessensalina, A., "An Empirical Evaluation of Supervised Learning in High Dimensions," *Proc. of the 25th International Conference on Machine Learning*, pp. 96-103, 2008.
13. Viola, P. and Jones, M., "Rapid Object Detection using a Boosted Cascade of Simple Features," *Proc. of IEEE Computer Society Conference on Computer Vision and Pattern Recognition*, Vol. 1, pp. 511-518, 2001.
14. Crow, F. C., "Summed-Area Tables For Texture Mapping," *ACM SIGGRAPH Computer Graphics*, Vol. 18, No. 3, pp. 207-212, 1984.
15. Ozuysal, M., Calonder, M., Lepetit, V., and Fua, P., "Fast Keypoint Recognition using Random Ferns," *IEEE Transactions on Pattern Analysis and Machine Intelligence*, Vol. 32, No. 3, pp. 448-461, 2010.
16. Shumin, D., Zhoufeng, L., and Chunlei, L., "AdaBoost Learning for Fabric Defect Detection based on Hog and SVM," *Proc. of International Conference on Multimedia Technology*, pp. 2903-2906, 2011.
17. Cord, A. and Chambon, S., "Automatic Road Defect Detection by Textural Pattern Recognition based on AdaBoost," *ComputerAided Civil and Infrastructure Engineering*, Vol. 27, No. 4, pp. 244-259, 2012.
18. Freund, Y. and Schapire, R. E., "A Decision-Theoretic Generalization of On-Line Learning and an Application to Boosting," *Journal of Computer and System Sciences*, Vol. 55, No. 1, pp. 119-139, 1997.
19. Teng, Z. and Kang, D. J., "Disjunctive Normal Form of Weak Classifiers for Online Learning based Object Tracking," *Proc. of the International Conference on Computer Vision Theory and Applications*, Vol. 2, pp. 138-146, 2013.
20. Yang, K., "Anytime Synchronized-Biased-Greedy Rapidly-Exploring Random Tree Path Planning in Two Dimensional Complex Environments," *International Journal of Control, Automation and Systems*, Vol. 9, No. 4, pp. 750-758, 2011.
21. Helen, R. and Kamaraj, N., "CAD Scheme To Detect Brain Tumour In MR Images using Active Contour Models and Tree Classifiers," *Journal of Electrical Engineering and Technology*, Vol. 10, No. 2, pp. 670-675, 2015.
22. Canny, J., "A Computational Approach to Edge Detection," *IEEE Transactions on Pattern Analysis and Machine Intelligence*, Vol. PAMI-8, No. 6, pp. 679-698, 1986.
23. Benaicha, A., Mourrot, G., Benothman, K., and Ragot, J., "Determination of Principal Component Analysis Models for Sensor Fault Detection and Isolation," *International Journal of Control, Automation and Systems*, Vol. 11, No. 2, pp. 296-305, 2013.